Study of Flow Pressure Characteristics of Improved Rotary Valve

Wenhua JIA*, Chenbo YIN**, Guo LI***, Dasheng ZHU****, Yanyan LIU*****, Shen DING******

*School of Mechanical Engineering, Nanjing Institute of Technology, China, E-mail: geovrml@163.com (Corresponding author)
**School of Mechanical and Power Engineering, Nanjing University of Technology, China, E-mail: chenboyin@163.com
***School of Mechanical Engineering, Nanjing Institute of Technology, China, E-mail: 61574544@qq.com
****School of Mechanical Engineering, Nanjing Institute of Technology, China, E-mail: 76062767 @qq.com
*****School of Mechanical Engineering, Nanjing Institute of Technology, China, E-mail: 2830194214 @qq.com
*****School of Mechanical Engineering, Nanjing Institute of Technology, China, E-mail: 1426858696 @qq.com

1. Introduction

The electro-hydraulic servo rotary valve [1, 2] is a type of direct-acting electro-hydraulic servo valve that drives the valve core to rotate directly or indirectly to achieve the opening and closing, reversing, and flow adjustment of the oil circuit. The rotary valve could control the small flow rate with high resolution, no acceleration and zero drift of the core movement, high control accuracy, and as the rotary core being directly driven by the motor, a compact structure, stronger anti-pollution characteristics, and other features. The rotary movement of the hydraulic rotary valve core could be realized in many ways, such as through servo motors and hydraulic motors. Compared with the hydraulic sliding valve, the hydraulic rotary valve had the advantages of simple structure, high working frequency, high reliability, and low sensitivity to oil pollution. Therefore, it is being increasingly applied to engineering problems. Some hydraulic pressure drove the main core, and the spiral groove was used to generate a pressure difference in the valve cavity to act as the driving force in [3], which is a rotary valve that could achieve large flow control, laying the foundation for future valve development. For the rotary valve [4] used in the hydraulic power assist system of automobile rudder, the core was round-toothed, and the core and valve sleeve were processed with symmetrical radial oil through holes whose symmetrical structure made the radial force on the valve core balanced. For the single-degree-of-freedom rotary valve [5], the driving core was provided symmetrically with two long grooves, using the hydraulic pressure drive, and the long grooves on the driving core were easier to process than the spiral groove [6]. For an electro-hydraulic servo rotary valve [7], the inner hole of the stacked metal discs was formed by photo etching. Different discs could be arranged in the valve sleeve into the flow channel with blind holes in different directions to make the rotary valve power level structure more compact. In literature [8], the angle of the disc valve port was optimized. By changing the size of the jet angle, the hydraulic power could be reduced. For a rotary valve with six groups of valve holes arranged symmetrically along the radial direction [9] on the sleeve, the valve core had a small mass, small inertia force, and low driving torque. Literature [10] compared the various clamping phenomena of the rotary valve and the sliding valve cores, and focused on the theoretical analysis of the radial imbalance force of the rotary valve, and proposed some specific measures to reduce the clamping phenomena

of the rotary valve, which provided the foundation for the optimal design of the rotary valve. The rotary valve of the sector valve port formed on the O-type groove valve core [11, 12] could cover the rectangular hole on the valve sleeve and meet the linear flow rate, laying the foundation for the structural improvement of the core. But the radial force was unbalanced, with small rated flow which was easy to cause cavitation.

Bending machine is important for sheet metal manufacturing equipment, which is widely used in manufacturing industries such as vehicles, airplanes, and electrical appliances. The movement of this machine is realized by the cylinders.

The purpose of this paper is to optimize the core component, rotary valve of a digital cylinder used in bending machine to improve the characteristics of the rotary valve and make the bending machine move stability. Firstly, by calculating the flow area of the valve port of the rotary valve, it was found that the O-type valve port had an excessively large gradient of co-flowing area when the opening was relatively small, which might cause the occurrence of reversing shock, vibration, and other failures. Secondly, on the basis of the O-type valve port, the V-type throttling groove valve port (V+O-type) was connected in parallel, and the processing method of the V-shaped throttle groove was analyzed. And then, under different opening angles, this study compared and analyzed the steady-state flow field outlet velocity, outlet jet angle, and outlet pressure of the rotary valve with O-type valve port and rotary valve with V+O-type throttling groove valve port, and concluded that the V+O-type throttling groove valve port had better flow field characteristics.

2. Analysis of the structure and flow area of the valve port of the rotary valve

The rotary valve operated based on the principle of changing the dimensions of the valve port opening by changing the relative position of the valve core and valve body, thereby varying the direction and size of the hydraulic oil flow. The rotary directional valve (rotary valve) shown in Fig.1 had a core that could rotate freely in the valve body without axial displacement. The rotation of the core accomplished the connection of various oil passages or blocking the relative movement between the core and the valve body. Fig. 2 was the schematic diagram model of the three-dimensional structure of the rotary valve core and valve body. The

schematic diagram of the relative movement was shown in Fig. 3 to complete the telescopic action of the hydraulic cylinder.
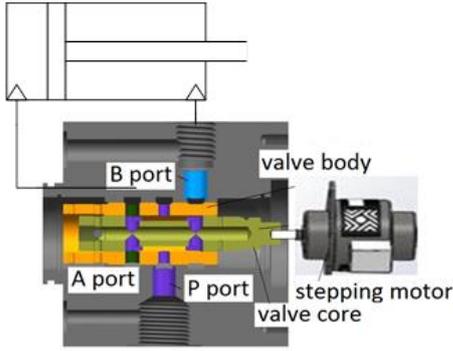

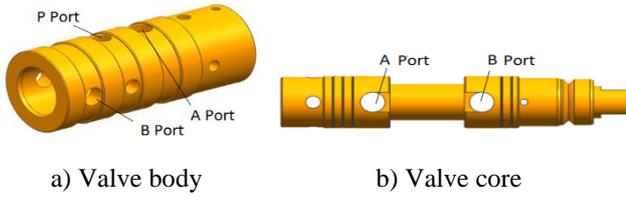Fig. 1 Schematic of working principle of rotary valve

a) Valve body

b) Valve core

Fig. 2 Model of valve body and valve core

2.1. O-type valve port design analysis

The schematic diagram of valve core rotation relative to the valve body is shown in Fig. 3. As shown in Fig. 3, the P port is connected with the A port. θ is the relative rotated angle of valve core and valve body. When the angle was equal to 0, port A and P were completely closed and the overflow area was 0. The valve body was fixed relative to the valve core and did not rotate. The valve core rotated clockwise relative to the valve sleeve. When the angle θ was greater than 0 and less than 45°, the fluid entered port A through port P. As shown in Fig. 4, the flow area gradually increased to the maximum when the angle was 45°, and the valve core continued to rotate. When the angle was greater than 45° and less than 90°, the area decreased gradually. When the angle was 90°, the flow area decreased to 0.
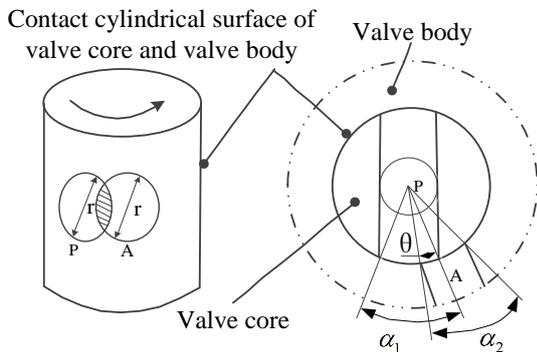

Fig. 3 Flow area diagram of rotary valve

The flow area of the rotary valve was closely related to the effective performance area of the core and the displacement of the core. As shown in Fig. 3, the two circles in the figure represent the core and body ports, respectively. The shadow of these two circles represents the flow area of the valve port.

Then, the flow area of the circular valve port was expressed as follows:

$$A(\theta) = 0, \quad \theta \in \left[0, \frac{\alpha_2 - \alpha_1}{2}\right), \tag{1}$$

$$A(\theta) = \frac{r^2}{2}\left[\left(\frac{\pi}{4}\right)^2 arccos\left(1 - \frac{4\theta}{\pi}\right) - \left(\frac{\pi}{4} - \theta\right)\sqrt{\theta\left(\frac{\pi}{2} - \theta\right)}\right], \tag{2}$$

$$\theta \in \left[\frac{\alpha_2 - \alpha_1}{2}, \frac{\pi}{4}\right)$$

$$A(\theta) = \frac{r^2}{2}\left[\left(\frac{\pi}{4}\right)^2 arccos\left(\frac{4\theta}{\pi} - 1\right) - \left(\theta - \frac{\pi}{2}\right)\sqrt{\theta\left(\frac{\pi}{2} - \theta\right)}\right], \tag{3}$$

$$\theta \in \left[\frac{\pi}{4}, \frac{\alpha_2 + \alpha_1}{2}\right)$$

$$A(\theta) = 0, \quad \theta \in \left[\frac{\alpha_2 + \alpha_1}{2}, \frac{\pi}{2}\right]. \tag{4}$$
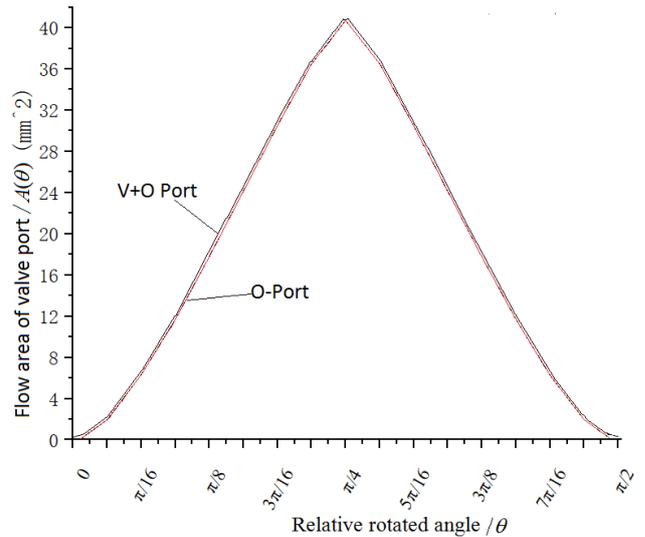

Fig. 4 Curves of flow area and relative rotated angle

$A(\theta)$ is the flow area of the circular valve port. $r = D/2$. D is the diameter of the contact surface of the valve core and body. Substitute the data about O-type port valve in Table 1 into formula (1), the flow area of the rotary valve port was proportional to the square of the radius of the valve core. According to the working principle of the rotary valve, the valve core matched with the valve sleeve from the opening to the closing of the valve, and the rotated angle of the valve core was $\pi/2$. Then the flow area of the valve port was obtained, as shown in Fig. 5 (O-type Port). The angle of rotation of the valve core was from 0 to $\pi/2$. During this period, the flow area was the largest when the angle of rotation was $\pi/4$. During the process from the opening to the closing of the valve core, the opening of the valve reached the maximum when the angular displacement of the valve core was

$\pi/4$. Also, the flow area reached the maximum value, which was approximately 40 mm^2. When the angular displacements of the valve core were 0 and $\pi/2$, the valve port was closed. At this time, the flow area was also 0.
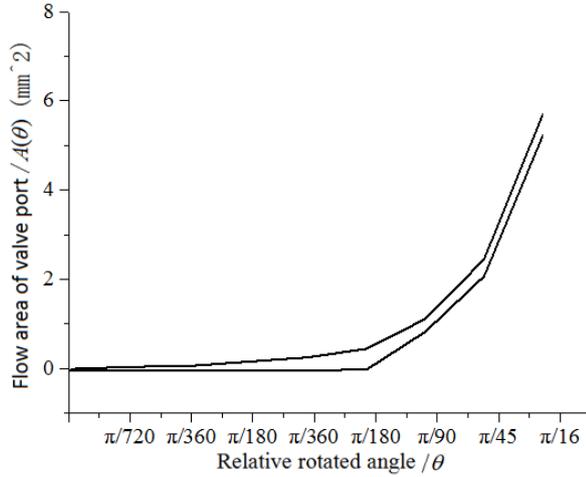

Fig. 5 Partial enlarged curves of flow area

2.2. V+O-type rotary valve port with V-groove design

As shown in Fig. 2, the valve core port and valve body port of the traditional rotary valve were both O-type. and the flow area gradient of the valve port was still very large when the valve port was about to close. The essence was that the first derivative of the flow area $A(\theta)$ compared to the relative rotation angle θ of the valve core and body (that is, the flow area gradient) was too large when the port was about to open or close. The high flow gradient meant that the flow area increased rapidly when the opening was relatively small, which might cause unpredictable accidents. As a reference, the vane of the vane pump [13, 14] had a V-shaped groove with a triangular cross section from the oil seal area into the end of the oil pressure area, connecting the closed liquid oil of the two vanes to the pressure oil through the V-shaped groove before entering the pressure oil area. Through the damping effect of the V-shaped groove, the pressure gradually rose, thus slowing down the flow and pressure pulsation and reducing the noise. Therefore, in this section, the V+O-type throttling groove rotary valve port was designed after considering the characteristics of the O-type valve port. The reversing valve was a front cover valve with a certain dead zone. After including the V-shaped throttling groove, the dead zone was reduced or even disappeared.

Using angle forming cutting tools such as symmetrical angle milling cutters, a V-shaped throttling groove was opened on both sides of the O-shaped valve port of the valve core, resulting in zero dead zone in the valve port, while other structures and parameters of the valve port were intact. The valve port with V-groove is shown in Fig. 6. The processing schematic diagram of the V-shaped throttling groove and its partial enlargement are shown in Fig. 7.

In Fig. 7 D is the diameter of the contact surface of the valve core and sleeve; D_1 is the diameter of the upper and lower valve ports of the valve core; α is the cutting edge angle of the milling cutter; H is the depth of cut of the milling cutter; d is the diameter of the milling cutter; T is the thickness of the milling cutter; a is the center distance; α_C is the central angle corresponding to the V-shaped throttling groove. α_1 is the central angle corresponding to port P of valve body. α_2 is the central angle corresponding to Port A of valve core.

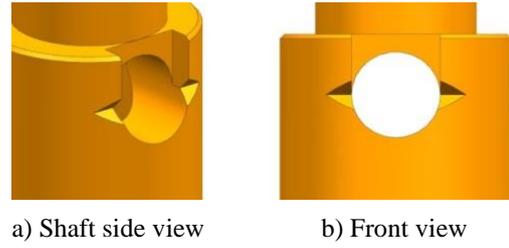a) Shaft side view   b) Front view
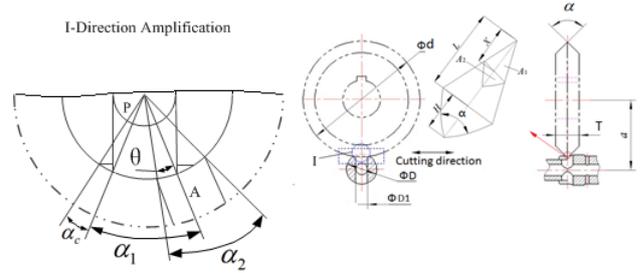
Fig. 6 Valve port with V- groove

Fig. 7 Schematic diagram of valve port with V- groove

$$\begin{cases} H = \dfrac{2 - \sqrt{2 + \sqrt{2}}}{2} D \\ L = \dfrac{D}{2} \cdot \alpha_C \\ \alpha_C = arccos\left(\dfrac{D_1}{D} + \dfrac{\sqrt{2 + \sqrt{2}}}{2} - 1\right) - arcsin\dfrac{D_1}{D} \end{cases} \quad . \quad (5)$$

The characteristic size of the V-type throttling groove is much smaller than the diameter of the valve core, and the cross-sectional areas of the V-type throttling groove A_1 and A_2 are shown in the following formula (6) and (7). This flow area was $A(\theta)$.

$$\begin{cases} A_1 = \dfrac{X^2}{L} \cdot H \cdot tan\dfrac{\alpha}{2} \cdot \dfrac{180 \cdot \theta}{\pi \cdot \alpha_C}, \theta \in \left[\dfrac{\alpha_2 - \alpha_1}{2}, \alpha_C\right] \\ A_2 = \left(\dfrac{H}{L} \cdot X\right)^2 \cdot tan\dfrac{\alpha}{2} \cdot \dfrac{180 \cdot \theta}{\pi \cdot \alpha_C}, \theta \in \left[\dfrac{\alpha_2 - \alpha_1}{2}, \alpha_C\right] \end{cases}, \quad (6)$$

$$A(\theta) = min(A_1, A_2), \quad \theta \in \left[\dfrac{\alpha_2 - \alpha_1}{2}, \alpha_C\right]. \quad (7)$$

Table 1

Parameters of O-type and V+O-type rotary valve

Parameters	D_1, mm	D, mm	D_2, mm	α_1, degree	α_2, degree	α_C, degree
O-type	4.95	13.5	4.95	42.2615°	45°	0
V+O-	4.95	13.5	4.95	42.2615°	45°	0.9898

The specific parameters for setting the valve ports were shown in Table1. Diameter D was 13.5 mm, the cutting edge angle α of the milling cutter was 90° and the diameter d of the milling cutter was 50 mm, and using the data of

V+O-type port in Table1. By substituting these data into formula (7) and formula (1)-(4), the flow area of the optimized rotary valve with V throttle groove was obtained, as shown in Fig. 4. The flow area of the improved V+O-type port valve with relative rotated angle from 0 to α_C was shown in Fig. 5. Comparing the two curves in Figs. 4 and 5, the trend of the two curves is basically the same. But flow area of V+O-type port rotary valve does not increase sharply at the moment of valve opening, due to the addition of V-type throttling groove.

3. Simulation analysis of flow field of the rotary valve

In this section, the flow field of the rotary valve was analyzed using FLUENT software. Traditional unstructured grid generation method was used in this software. The construction fluid was an incompressible Newtonian fluid, and the pressure solver and the steady-state solver were used. The turbulence model was used and the standard model of *k-epsilon* equation turbulence was used. The fluid medium is oil-860, the density is 860 kg/m³ and the viscosity is 0.036 kg/(m.s). It was assumed that there was no temperature rise of the fluid, and the influence of the temperature rise of the fluid was not considered. The boundary conditions and medium temperature were set as the initial values. The inlet pressure was 25 MPa, while the outlet pressure was 23 MPa. The residual error in all directions was set to 0.0001mm. After the initialization, the number of iterations of the calculation was set to 2000.

3.1. Outlet velocity characteristics of flow fields with constant pressure difference

When the opening angles of the rotary valve were the same and the inlet and outlet pressure difference was set to a fixed value, the study analyzed the pressure field and velocity field distribution within the rotary valve, carrying out direct comparison and analysis of the rotary valve with V-type throttling groove valve port and rotary valve with the O-type valve port with the same opening angles.
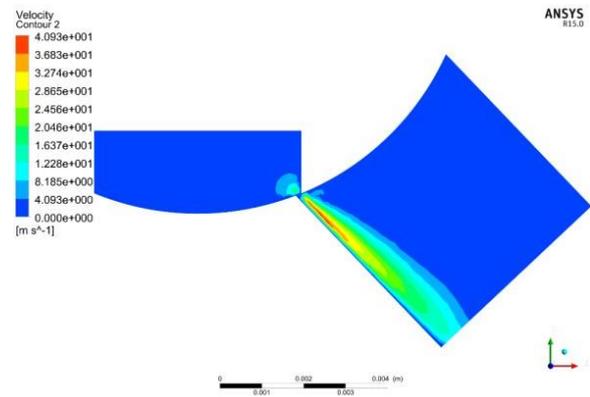
The flow field model when the angular displacement of the O-shaped valve port that was the rotation angles θ was 1.5° to 45° was established. The outlet velocity nephogram was shown in Fig. 8.

As shown in Fig.7, when the core angle was relatively small, the maximum flow rate in the O-shaped valve port flow field opening occurred at the lower left wall surface of the valve port of the valve body. As the core opening increased, the maximum flow rate started to occur at the intersection of the core, port, and body.
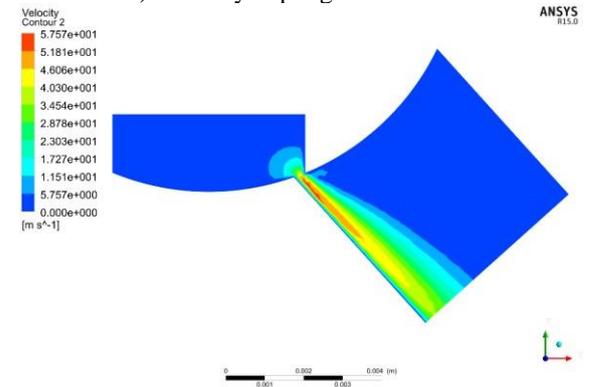
The flow field models of the V+O-type rotary valve at the rotation angles θ of 1°, 4°, 24° and 45° were respectively established. The outlet velocity nephogram was shown in Fig. 9.

From the overall view of Fig. 9, when the rotation angle was 1°, the V+O valve port was at the junction between the V-type throttling groove and the O-type port, and the maximum hydraulic oil flow rate occurred at the opening, at about 49.6m/s, and the jet angle was relatively small. When the angle of rotation was 4°, the V+O-type throttling groove valve port had a higher maximum outlet flow rate than the O-type valve port, but the proportion of the area where the flow rate changed drastically was significantly smaller than that of the O-type valve port. When the rotation
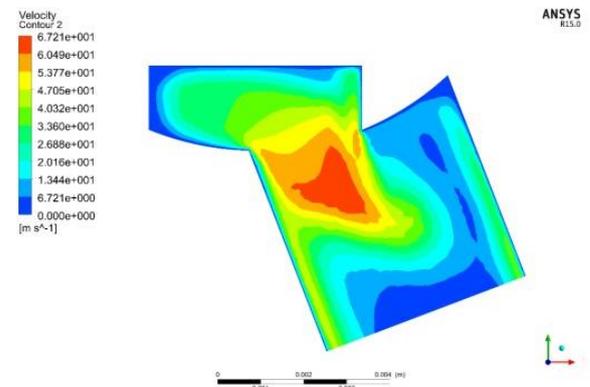
of the core was up to 45°, the maximum velocity difference between the V+O-type throttle groove and the O-type valve port flow fields was small. Therefore, while the V-type
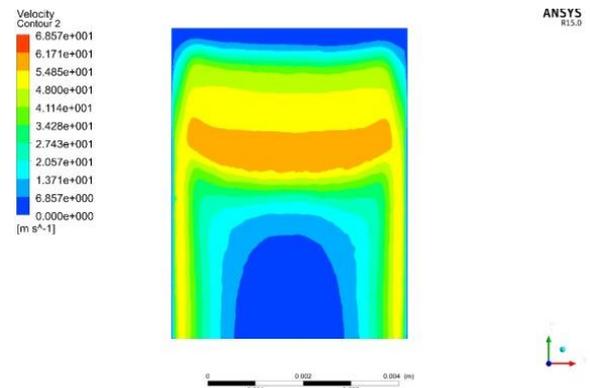

a) Velocity nephogram at θ=1.5°

b)Velocity nephogram at $\theta = 4°$

c) Velocity nephogram at θ =24°

d) Velocity nephogram at $\theta = 45°$

Fig. 8 O-type of velocity nephogram

throttling valve port obviously limited the flow rate with opening at a small angle, it could ensure that with opening at a large angle, the characteristics including the highest flow rate were close to that of the O-type valve port, which satisfied the design requirements.
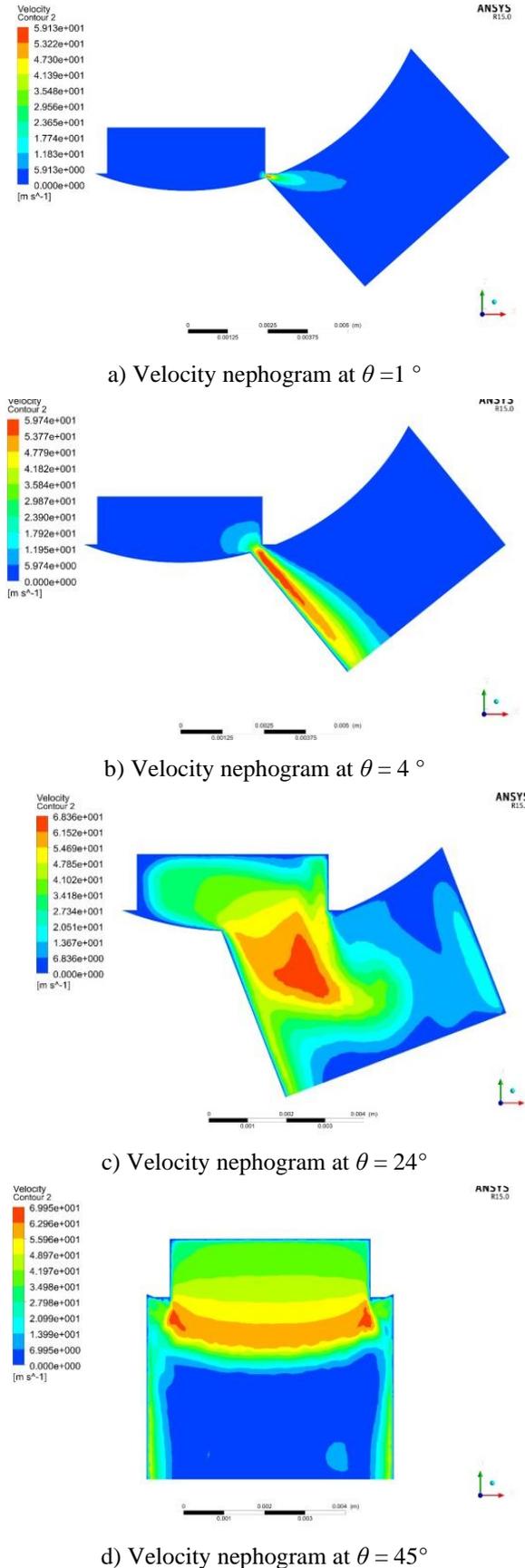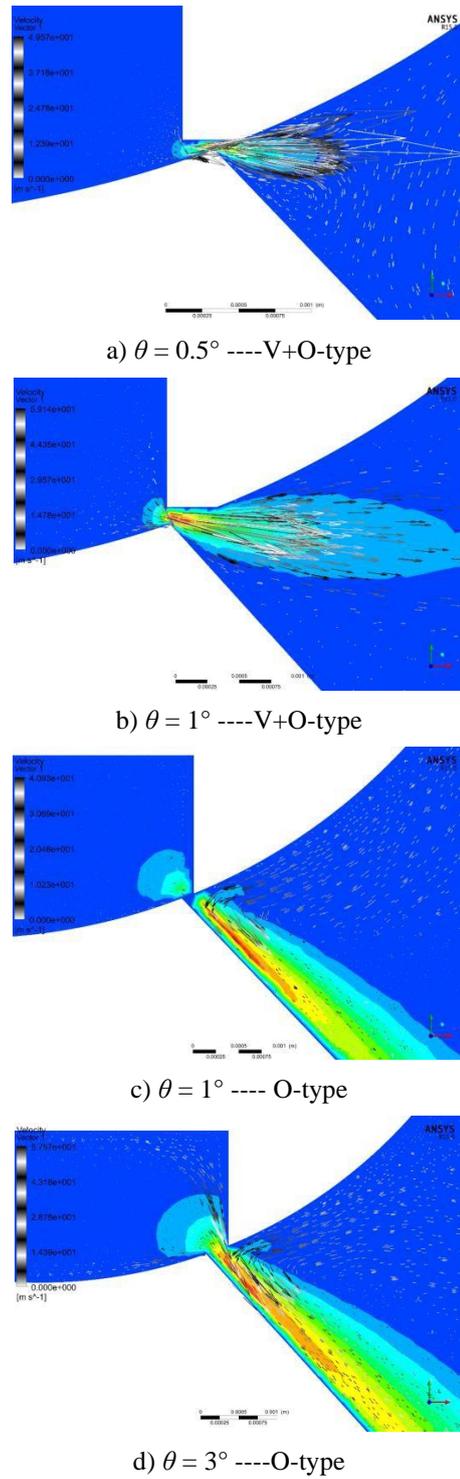

a) Velocity nephogram at $\theta = 1°$

b) Velocity nephogram at $\theta = 4°$

c) Velocity nephogram at $\theta = 24°$

d) Velocity nephogram at $\theta = 45°$

Fig. 9 Velocity nephogram of rotary valve with V-port

a) $\theta = 0.5°$ ----V+O-type

b) $\theta = 1°$ ----V+O-type

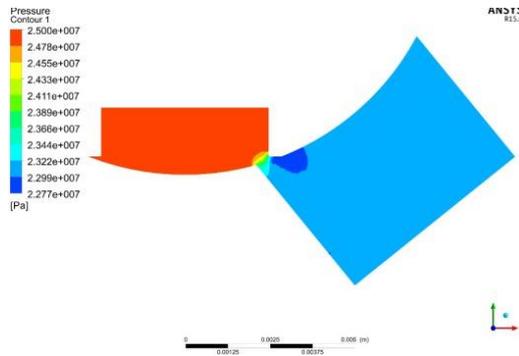c) $\theta = 1°$ ---- O-type

d) $\theta = 3°$ ----O-type

Fig. 10 Enlarged view of velocity nephogram

When the rotation angles were 0.5° and 1°, the enlarged velocity vector diagram of the flow field outlet position of the V+O type throttling groove of the valve port is shown in Fig. 10. From the in-plane velocity vector diagram of the flow field (Figs. 10, a and b), it can be seen that the jet angle of the V+O-port valve when the core opening was relatively small were about 5° and 15°. But further analysis of the jet angle from the enlarged velocity vector diagram (Figs. 10, c and d) showed that the jet flow phenomenon was more obvious when the relative rotated angle θ was relatively small, the jet angle reached approximately 50°. After adding the V-type throttling groove, the throttling characte-
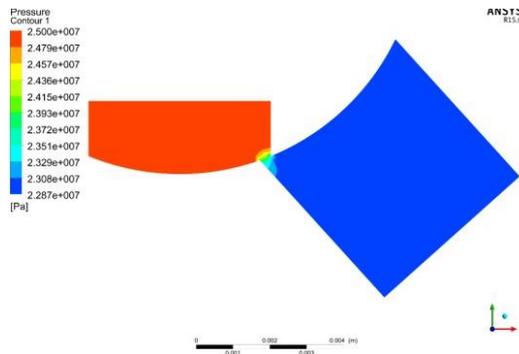
ristic of the valve port at the initial stage was obviously better than that of the traditional O-type valve port.

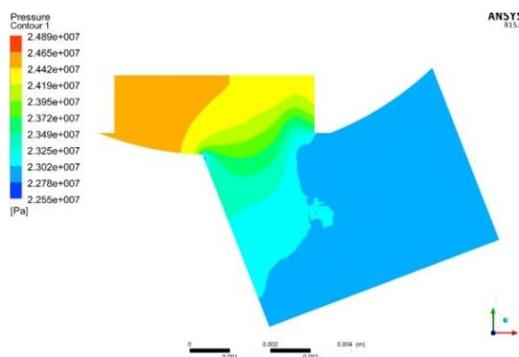### 3.2. Outlet pressure characteristics of flow fields with constant pressure difference

The initial setting remained unchanged, and the comparison of the pressure nephogram of the flow fields between the V+O-type throttling groove valve port and the O-type valve port is shown in Fig. 11.
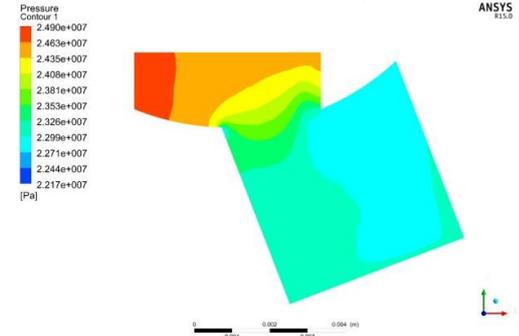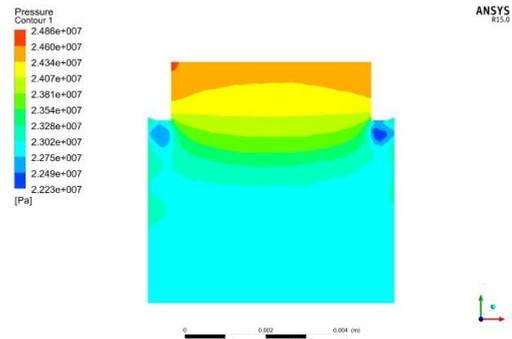
a) θ= 3° of V+O-type

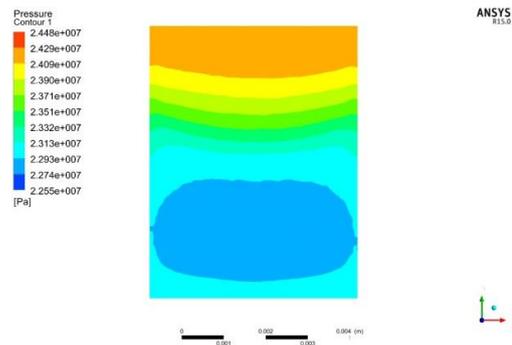b) θ= 3° of O - port

c) θ= 24° of V+O - type

d) θ= 24° of O – port

Fig. 11 Pressure nephogram

e) θ= 45° of V+O -port

f) θ= 45° of O- port

Fig. 11 Continuation

As shown in Fig. 11, when the core rotation angle was relatively small (3°), the V+O-type throttling groove valve port had a smaller pressure change area than the O-type valve port, with a pressure reduction effect of approximately 0.04 MPa. When the openings were 24° and 45°, the proportion of the negative pressure zone of the O-type valve port further enlarged, 50% of the area was negative pressure area. Although the valve port of the V+O-type throttling groove port also had a small proportion of the negative pressure zone, the proportion of the negative pressure zone was significantly smaller than the O-type valve port.

4. Conclusions

The V+O type throttling groove rotary valve port was designed after considering the characteristics of the O type valve port. After research, it can be determined that the V+O-type throttle groove valve port had better pressure performance than the O-type valve port, and in particular, it was significantly better than the O-type valve port in reducing the proportion of the negative pressure area.

1. At the initial opening of the valve core, when the rotation angle was 1°, the maximum hydraulic oil flow rate is about 49.6 m/s. The V+O-port valve had a higher outlet flow rate than the O-type valve port, but the proportion of the area where the flow rate changed drastically was significantly smaller than that of the O-type valve port. When the opening was relatively large, the flow rate characteristics were not much different. In terms of jet angle, it had a significant impact on the change in jet angle, which was much smaller than the jet angle of a single O-type valve port. When the rotation angles was 1°, the jet angle of the V+O-port valve was 15°, but the O port was close to 50°.

2. The V+O type multi-stage throttling groove valve port had a smaller pressure change area than the O

type valve port when the opening was relatively small, was approximately 0.04 MPa. As the opening increased, such as was 45°, the single-stage O type valve port began to have a large negative pressure zone, 50% of the area was negative pressure area, while the V +O-type multi-stage valve port had no obvious negative pressure zone, and the larger the opening, the more the proportion of the O-type valve port negative pressure zone. It can be concluded that the V+O type valve port was significantly better than the single O type valve port and could effectively suppress the occurrence of cavitation and other faults.

Acknowledgement

References

1. **Yuan, J. Y.; Yin, Y. B.; Lu, L.; Fang, X.; Guo, S. R.** 2018. Analysis of rotary direct drive electro-hydraulic pressure control servo valve, Journal of Mechanical Engineering 54(16): 186-194. (in Chinese).
   http://dx.doi.org/10.3901/JME.2018.16.186.

2. **Wang, H., Quan, L.; Huang, J. H.; Gong, G. F.; Yang, Y.** 2019. Reduction of steady flow torques in a single-stage rotary servo valve, Proc. I. Mech. Eng. E-J. Pro. 233(4): 718-727.
   http://dx.doi.org/10.1177/0954408918793402.

3. **Karem, A.; Siamak, N.; Dupac, M.; Godfry, P.** 2019. A dynamic model and performance analysis of a stepped rotary flow control valve, Proc. I. Mech. Eng. I-J. SYS. 233(9): 1195-1208.
   http://dx.doi.org/10.1177/0959651818820978.

4. **Petukhov, D; Korn, L.; Walter, M.; Telyshev, D.** 2019. A novel control method for rotary blood pumps as left ventricular assist device utilizing aorticvalve state detection, Biomed Research International, 2019.
   http://dx.doi.org/ 10.1155/2019/1732160.

5. **Pournazeri, M.; Khajepour, A.; Huang, Y. J.** 2017. Development of a new fully flexible hydraulic variable valve actuation system for engines usingrotary spool valves, Mechatronics 46:1-20.
   http://dx.doi.org/10.1016/j.mechatronics.2017.06.010.

6. **Wu, S.; Jiao, Z. X.; Yan, L.; Zhang, R.; Yu, J. T.; Chen. C. Y.** 2014. Development of a direct-drive servo valve with high-frequency voice coil motor and advanced digital controller, IEEE-ASME Transactions on Mechatronics 19(3): 932-942.
   http://dx.doi.org/10.1109/TMECH.2013.2264218.

7. **Tu, H.C; Rannow, M. B; Wang, M.; Li, P. L; Chase, T. R.; Van de Ven, J. D.** 2012. Design, modeling, and validation of a high-speed rotary pulse-width-modulation on/off hydraulic valve. Journal of Dynamic Systems, Measurement, and Control 134(6): 061002.
   http://dx.doi.org/10.1115/1.4006621.

8. **Zaryankin, A. E.; Zaryankin, V.A.; Akatov, A.S.** 2020. Development and investigation of a new rotary valve for power steam turbines. Thermal Engineering 67: 249–255.
   http://dx.doi.org/10.1134/s0040601520050109.

9. **Liu, N.; Liu, Z. L.; Li, Y. X.; Sang, L. X.** 2016. Development and experimental studies on a fully-rotary valve energy recovery device for SWRO desalination system, Desalination 397: 67-74.
   http://dx.doi.org/10.1016/j.desal.2016.06.026.

10. **Ren, Y.; Ruan, J.** 2016. Theoretical and experimental investigations of vibration waveforms excited by an electro-hydraulic type exciter for fatigue with a two-dimensional rotary valve, Mechatronics 33:161-172.
    http://dx.doi.org/10.1016/j.mechatronics.2015.12.006.

11. **Yan, Z. D.; Wei, C. M.; Geng, Y. F.; Shao, J.; Hu, X. F.; Li, Y.** 2015. Design of a rotary valve orifice for a continuous wave mud pulse generator, Precision Engineering-Journal of the International Societies for Precision Engineering and Nanotechnology 41:111-118.
    http://dx.doi.org/10.1016/j.precisioneng.2015.03.005.

12. **Zhu, M. Z.; Zhao, S. D.; Dong, P.; Li, J. X.** 2018. Design and analysis of a novel double-servo direct drive rotary valve with high frequency. Journal of Mechanical Science and Technology 32: 4313–4323.
    http://dx.doi.org/10.1007/s12206-018-0829-x.

13. **Wu, T. C.; Andres, L. S.** 2019. Pump grooved seals: a computational fluid dynamics approach to improve bulk-flow model predictions, Journal of Engineering for Gas Turbines and Power-Transactions of the ASME 141(10): 101005
    http://dx.doi.org/10.1115/1.4044283.

W. Jia, C. Yin, G. Li, D. Zhu, Y. Liu, S. Ding

STUDY OF FLOW PRESSURE CHARACTERISTICS OF IMPROVED ROTARY VALVE

S u m m a r y

This paper presents flow pressure characteristics of O-type rotary valve. After calculating the flow area of the O-type valve port, this study found that the area gradient was still relatively large when the opening was small. When the rotation angles were small, the jet angle of the V+O-port valve was significantly smaller than the O-type's. The proportion of the O-type valve port negative pressure zone was obviously larger than the single V+O- type rotary valve.